A Numerical Investigation of Local Effects on the Global Behavior of TEHD Highly Loaded Circular Contacts

W. Habchi[1], P.Vergne[2], N. Fillot[2], S. Bair[3] and G. E. Morales-Espejel[4]

[1] Lebanese American University, Dep. of Ind. & Mech. Eng., Byblos, Lebanon
[2] Université de Lyon, CNRS, INSA-Lyon, LaMCoS UMR5259, F-69621, France
[3] G.W. Woodruff School of Mech. Eng., Centre for High Pressure Rheology, Georgia Institute of Technology, Atlanta, GA 30332-0405
[4] SKF Engineering and Research Centre, Nieuwegein, The Netherlands

Abstract

This paper presents a numerical investigation of the local behavior of highly loaded thermal elastohydrodynamic contacts. The study is a continuation to a previous work of the authors where it was found that neglecting the dependence of lubricants' thermal properties on pressure and temperature leads to an underestimation of friction coefficients under high sliding regime. In this work, the local phenomena behind these observations are investigated. The results suggest that a redistribution of heat from the center of the contact towards the environment is taking place, leading to globally lower temperatures inside the contact, which leads to higher friction coefficients.

1. Introduction

Ever since the first theoretical studies in elastohydrodynamic lubrication (EHL), comparisons of friction coefficients and film thickness predictions with experiments showed an important gap. It quickly became clear that for an accurate prediction of film thickness and especially friction in EHL conjunctions, it is mandatory to thoroughly account for the complex rheological behavior of lubricants under the severe operating conditions encountered in EHD contacts. Yet, until now, out of simplicity, most numerical works in EHL still employ basic rheological models such as a modification of the Barus [1] model or Roelands [2] model for viscosity-pressure dependence, or the Dowson & Higginson compressibility model and a restricted form of the Ree-Eyring [3] model for the shear-dependence of viscosity, even though there is a common agreement in the tribological community that these models fail to yield accurate predictions of film thickness and especially friction under mild or severe operating conditions. In addition, in most EHL studies which require a rheological component, the "non-

Newtonian" part is chosen from a menu of models without regard for the behavior which can actually be supported by primary measurements or for which sound theory exists. Both shear-thinning and a limit stress must be included in a high pressure simulation because both are aspects of shear response of liquids at very high shear stress [4]. The shear-thinning in simple liquids that can be described by a generalized Newtonian model is constitutive and results from molecular alignment, for example [5]. There is even good theory to predict the onset of shear-thinning [6]. The limiting stress is not constitutive since it results from slip within the film [7]. It is a form of liquid failure. A complete description of the response of a shear-thinning liquid would require differences between the normal stresses [6]. That is to say, the molecular alignment which causes shear-thinning results in the principal shear stress axes not being aligned with the principal shear axes. Therefore the plane within the film experiencing the greatest shear stress cannot be along the boundary and slip occurs within the film. Experimental high-pressure flow visualization shows the slip directions of which there must be two because there are two directions for which the shear stress is maximum [7].

Only recently, there has been a growing interest for including more realistic physically based rheological models [4] [8] in theoretical EHL predictions. For instance, in [9] the authors employed a thermal EHL approach to compute film thicknesses and friction coefficients in EHD contacts using the measured thermophysical properties of a reference liquid. Comparisons with experiments showed an excellent agreement over the considered range of operating conditions. This study provided useful insight on the thermal behavior of EHD contacts. However, the considered range of contact pressures was relatively mild to draw general conclusions. Other works in which a wider range of operating conditions were considered (e.g. see [10] and [11]) revealed that a full thermal analysis, including the pressure and temperature dependence of a lubricant's thermal properties, is necessary for an accurate prediction of film thickness and especially traction under severe operating conditions. Campos et al. [12] were able to obtain a fairly good agreement with experiments by adjusting the viscosity and by incorporating the pressure-dependence of the lubricant's thermal conductivity into their model while ignoring any temperature dependence of the latter and assuming a constant specific heat. Yet, under high mean entrainment speeds and sliding velocities, some discrepancies were observed. These could be attributed, in part, to the fact that the full pressure-temperature dependence of thermal properties of the lubricant was not considered in the analysis. The importance of accounting for the full temperature-pressure dependence of the lubricant thermal properties was also highlighted by Sharif et al. [13] [14] who included this dependence into their model based on the experimental data in [15] while also adjusting the viscosity. However, by adjusting the rheology, some of the thermal effects on friction may be incorrectly resolved. Recall that the sinh law originally came from viscous heating in capillary viscometers that was mistakenly attributed to thixotropy [16].

The current study comes as a continuation to the work published in [11] where the authors focused on the importance of accounting for the dependence of thermal properties of a lubricant on temperature and pressure in accurately predicting global contact parameters such as film thickness and friction in highly loaded EHD contacts. A typical mineral oil (Shell T9) was considered and the dependence of its transport properties on pressure and temperature was experimentally investigated. Appropriate analytical models were developed for these dependencies. The models were parameterized by primary measurements and included in a TEHL solver. The results suggested that neglecting the dependency of thermal properties on pressure and temperature has a negligible effect on film thickness under pure-rolling conditions. However, for traction calculation, neglecting this effect leads to an underestimation of friction coefficients compared to experiments. In this work, the authors propose a quantitative numerical investigation of the local phenomena behind these observations in order to reach a deeper understanding of the complex nature of the thermal elastohydrodynamic lubrication (TEHL) problem.

This work, like the previous paper, departs from the usual EHL simulation by employing measured transport properties including viscosity. Only the limiting stress was obtained from a contact measurement. Given the mounting importance of the reduction of mechanical loss in machinery to energy conservation and the attendant environment concerns, investigations which reveal the association of real liquid properties with friction must be greatly valued.

2. Lubricant thermophysical properties

The thermophysical properties of lubricant Shell T9 were discussed in detail in [11]. The variations of these properties with pressure, temperature and shear stress were measured and appropriate models were derived to represent these variations. The derived models are briefly recalled in the following. For further details, the interested reader is referred to [11] and references therein. Subscripts 0 and R indicate, respectively, ambient pressure and temperature ($p_0 = 0$ and $T_0 = 30^o\mathrm{C}$) and a reference state ($p_R = 0$ and $T_R = 25^o\mathrm{C}$).

2.1 Density

The Murnaghan [17] equation of state is used to model the density variation of lubricant Shell T9 with pressure and temperature:

$$\rho = \frac{\rho_R}{1 + a_V\left(T - T_R\right)} \times \left(1 + \frac{K_0'}{K_0}\, p\right)^{\frac{1}{K_0'}} \quad \text{with} \quad K_0 = K_{00} \exp\left(-\beta_K T\right) \qquad (1)$$

Where $K_0' = 10.545$, $a_V = 7.734 \times 10^{-4}\ \mathrm{K}^{-1}$, $K_{00} = 9.234\ \mathrm{GPa}$, $\rho_R = 875\, Kg/m^3$ and $\beta_K = 6.090 \times 10^{-3}\ \mathrm{K}^{-1}$ were obtained from experimental measurement.

2.2 Viscosity

A Vogel-like model with a thermodynamic scaling parameter is used to represent the pressure and temperature dependence of the viscosity of lubricant Shell T9:

$$\mu = \mu_\infty \exp\left(\frac{B_F \varphi_\infty}{\varphi - \varphi_\infty}\right) \quad \text{with} \quad \varphi = \left(\frac{T}{T_R}\right)\left(\frac{V}{V_R}\right)^g \tag{2}$$

Where $g = 5.0348$, $\varphi_\infty = 0.26844$, $B_F = 12.898$, and $\mu_\infty = 1.489 \times 10^{-4}$ Pa·s were obtained from experimental measurement. And from the Murnaghan equation of state:

$$\frac{V}{V_R} = \frac{1 + a_V (T - T_R)}{\left(1 + \frac{K_0'}{K_0} p\right)^{1/K_0'}} \tag{3}$$

As for the shear dependence of viscosity, the single-Newtonian modified Carreau-Yasuda equation [18] is used to define the generalized viscosity η as a function of shear stress τ as follows:

$$\eta = \frac{\mu}{\left[1 + \left(\frac{\tau}{G}\right)^a\right]^{\frac{\frac{1}{n} - 1}{a}}} \tag{4}$$

Where $G = 7.0$ MPa, $a = 5$ and $n = 0.35$ were obtained from experimental measurements. Finally, Shell T9 lubricant was shown to exhibit a limiting shear stress behavior under high shear rates. The limiting value of the shear stress τ_L was shown to depend on pressure according to:

$$\tau_L = \Lambda p \tag{5}$$

Where the limiting stress-pressure coefficient $\Lambda = 0.083$. This value was deduced from EHL traction experiments carried out under isothermal operating conditions.

2.3 Thermal properties

The thermal conductivity k and volumetric heat capacity $C = \rho c$ of Shell T9 were also measured [11] and their variations with temperature and pressure were represented by the following models:

$$k = B_k + C_k \kappa^{-s} \quad \text{with} \quad \kappa = \left(\frac{V}{V_R}\right)\left[1 + A\left(\frac{T}{T_R}\right)\left(\frac{V}{V_R}\right)^3\right] \tag{6}$$

$$\text{And } C = C' + m\chi \qquad \text{with} \qquad \chi = \left(\frac{T}{T_R}\right)\left(\frac{V}{V_R}\right)^{-4} \qquad (7)$$

Where $A = -0.101$, $B_k = 0.053 \text{Wm}^{-1}\text{K}^{-1}$, $C_k = 0.026 \text{Wm}^{-1}\text{K}^{-1}$, $s = 7.6$, $C' = 1.17 \times 10^6$ J/m$^3 \cdot$K and $m = 0.39 \times 10^6$ J/m$^3 \cdot$K were obtained from experimental measurements. The term V/V_R is obtained from equation (3).

3. Numerical model

The numerical model employed in this work was described in detail in [19] and [20]. In this section, only the main features of this model are recalled. An additional feature regarding the treatment of the Limiting Shear Stress behaviour is also described.

The model is based on a finite element fully-coupled resolution of the EHD equations: Reynolds, linear elasticity and load balance equations. The latter are solved simultaneously providing robust and fast converging solutions. The generalized Reynolds equation [21] is used to account for the shear dependence of the lubricant. Special formulations are introduced in order to stabilize the solution of Reynolds equation at high loads. The temperature distribution in the contact is obtained by solving the 3D energy equation in the lubricant film and solid bodies. An additional feature of the current model is that it incorporates the variations of the lubricant thermal properties with pressure and temperature throughout the contact. An iterative procedure is applied between the respective solutions of the EHD and thermal problems as described in [19] and [20]. However, in the current model a slight modification is introduced for the treatment of the Limiting Shear Stress behaviour of the lubricant. In fact, during the iterative procedure, every time the shear stress τ is evaluated (using viscosity data provided by a combination of the Carreau and Vogel-like models) it is either truncated to τ_L if it exceeds τ_L or, otherwise, it is kept unchanged.

4. Local investigation

In [11], it was shown that neglecting the dependency of thermal properties on pressure and temperature has a negligible effect on film thickness under pure-rolling conditions. However, for traction calculation, neglecting this effect leads to an underestimation of friction coefficients. In the following, it is proposed to investigate the local phenomena behind these observations. Steel-Steel circular contacts (ball-on-plane) are considered with a ball radius of 12.7mm. The surface of the plane corresponds to Z=0 whereas the sphere's surface corresponds to Z=1. The ambient temperature is taken to be T_0=30°C. Three different test cases denoted A, B, and C are considered. These cover a considerable range of load and mean entrainment speed conditions. The operating conditions for these cases are listed in Table 1.

Test Case	L (N)	p_h (GPa)	u_m (m/s)	u_s (m/s)	u_p (m/s)	SRR
A	38	0.85	0.8	1.20	0.40	1.0
B	154	1.35	2.0	3.00	1.00	1.0
C	250	1.59	2.5	3.75	1.25	1.0

Table 1: Operating conditions for the different test cases considered

Note that in test cases A, B and C the slide-to-roll ratio is kept constant (SRR=1.0) whereas the external applied load L and the mean entrainment speed u_m are gradually increased. Hence, the thermal severity of the contact is gradually increased leading to a more and more important power input to the contact zone and thermal dissipation as well. In order to assess the effect of the variations in thermal properties on the local behaviour of the contact, two sets of numerical results are considered. In the first set (referred to as "Constant C K"), thermal properties are kept constant (at their ambient pressure and temperature values), whereas in the second (referred to as "Variable C K"), they are allowed to vary with pressure and temperature according to the models presented in section 2.3. In the following, the local variations of different contact parameters such as thermal properties, temperature, heat generation etc. are studied throughout the contact. The variations of all properties across film thickness are shown at different locations (X=-1.0, X=-0.5, X=0.0 and X=0.5) along the central line (Y=0.0) of the contact.

4.1 Thermophysical properties

Figure 1 shows the variations of the dimensionless thermal conductivity k/k_0 across the film thickness for the "Variable C K" case only because for the "Constant C K" case k/k_0 is equal to 1 since k is not allowed to vary. Note that in all cases k/k_0 is greater than 1, indicating the increase in thermal conductivity of the lubricant as it passes through the contact. This is because both pressure and temperature increase in the contact area. In fact, the maximum value of k/k_0 is attained at the center of the contact (X=0.0) where maximum pressure and temperature values are encountered. And k/k_0 decreases as the lubricant moves away from the center of the contact. On the other hand, note that, in general, the lubricant's thermal conductivity is high around the midplane of the film (Z=0.5) and decreases when moving towards the solid surfaces. As a general observation, one can say that neglecting temperature and pressure dependence of thermal conductivity leads to an underestimation of heat removal by conduction from the contact area since thermal conductivity of the lubricant would be underestimated.

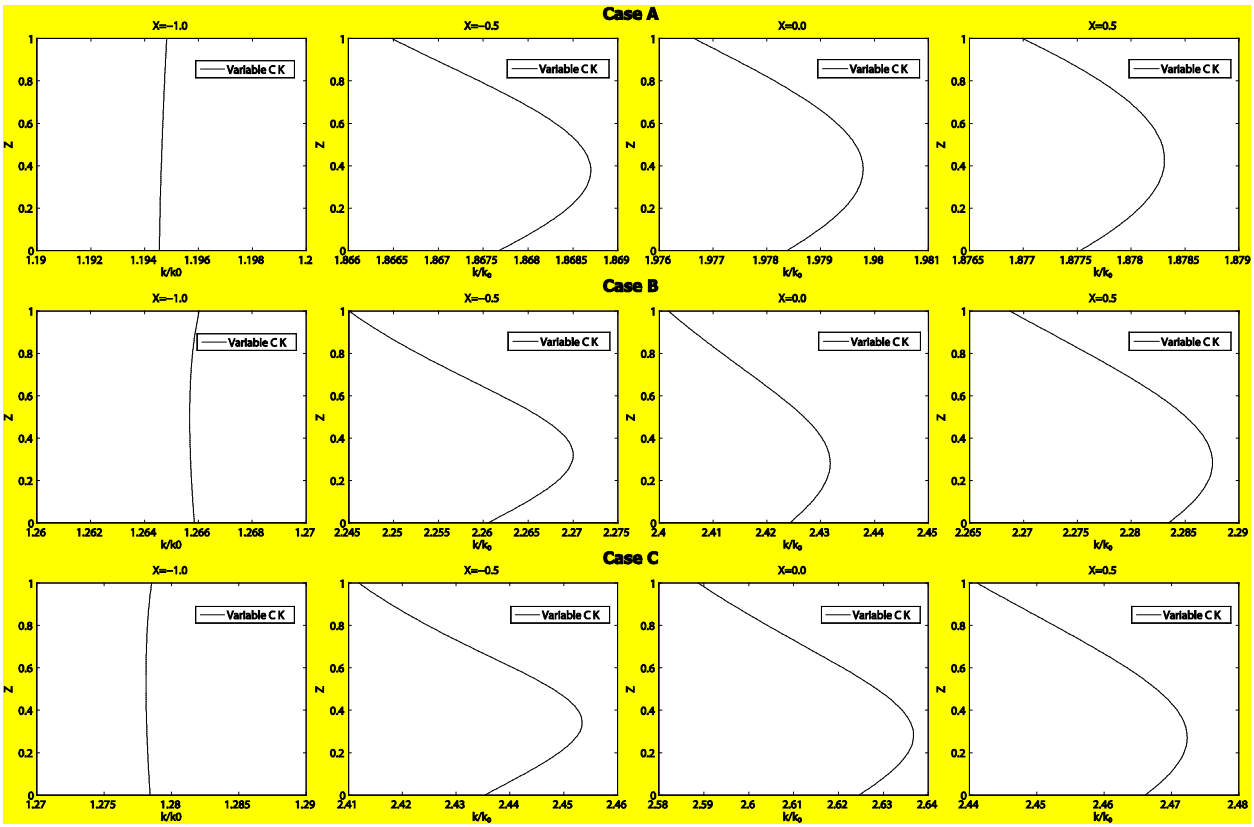

Figure 1: Thermal conductivity variations in the lubricant film thickness along the central line of the contact at different *X* locations

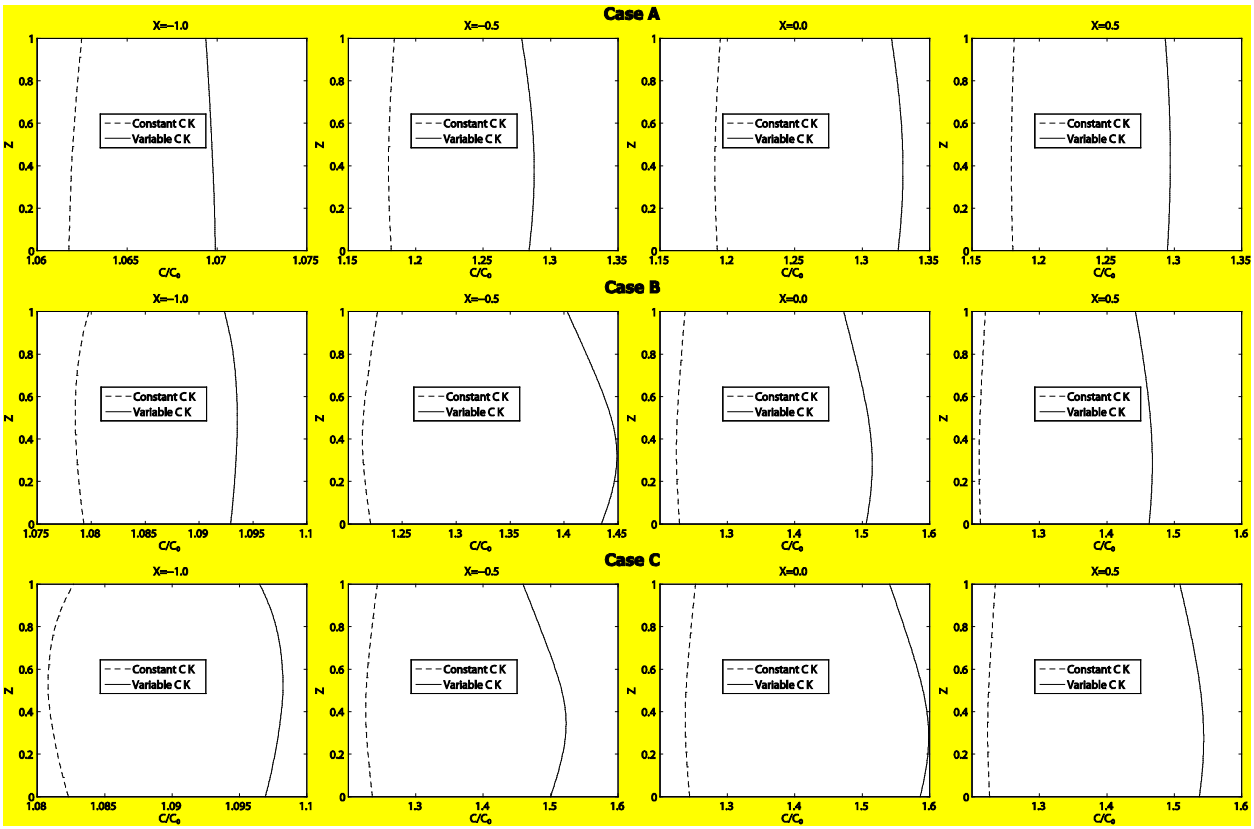

Figure 2: Volumetric heat capacity variations in the lubricant film thickness along the central line of the contact at different *X* locations

Figure 2 shows the variations of the dimensionless volumetric heat capacity C/C_0 across the film thickness for both the "Variable C K" and "Constant C K" cases. Note that for the "Constant C K" case, C/C_0 is not equal to 1 and as mentioned previously, it corresponds to ρ/ρ_0. Knowing that pressure is assumed to be constant throughout the film thickness, the variations of C/C_0 with Z in the "Constant C K" case correspond to the temperature-density dependence of the lubricant whereas the variations with X correspond to the pressure-temperature-density dependence. Figure 2 clearly shows an increase in the volumetric heat capacity C as the lubricant passes through the contact in both the "Constant C K" and "Variable C K" cases. However, this effect is more pronounced when the thermal heat capacity c is allowed to vary with pressure and temperature. Hence, neglecting the temperature and pressure dependence of the lubricant thermal properties also leads to an underestimation of heat removal from the contact by convection. Finally, note that in the "Variable C K" case, maximum values of C are observed around the midplane of the film rather than near the solid surfaces. This indicates that in this case, variations of C are dominated by the increase of the thermal heat capacity c with temperature around the midplane of the film, rather than the decrease of density ρ with increasing temperature in this area.

4.2 Temperature

Figure 3 shows temperature variations in the film thickness along the central line of the contact for both the “Constant C K” and “Variable C K” cases. It is clear that temperature increases as the fluid approaches the center of the contact (X=0.0) and then starts decreasing as the lubricant moves away from the contact area. This is because of the high viscosity encountered in this area, leading to high viscous power and thus high heat generation by shear. Hence, heat propagation takes place from the center towards the inlet and exit regions of the contact. In the film thickness, it is observed that the maximum temperature is found around the midplane of the lubricant film and temperature decreases near the solid surfaces indicating heat propagation form the middle of the film towards the solid components. However, note that at the plane’s surface (Z=0), temperature is always higher than at the sphere’s surface (Z=1). Knowing that the two solid surfaces are made out of the same material (Steel), this is expected since heat removal from the lubricant film by convection is more favorable on the sphere’s surface since it is moving at a higher speed.

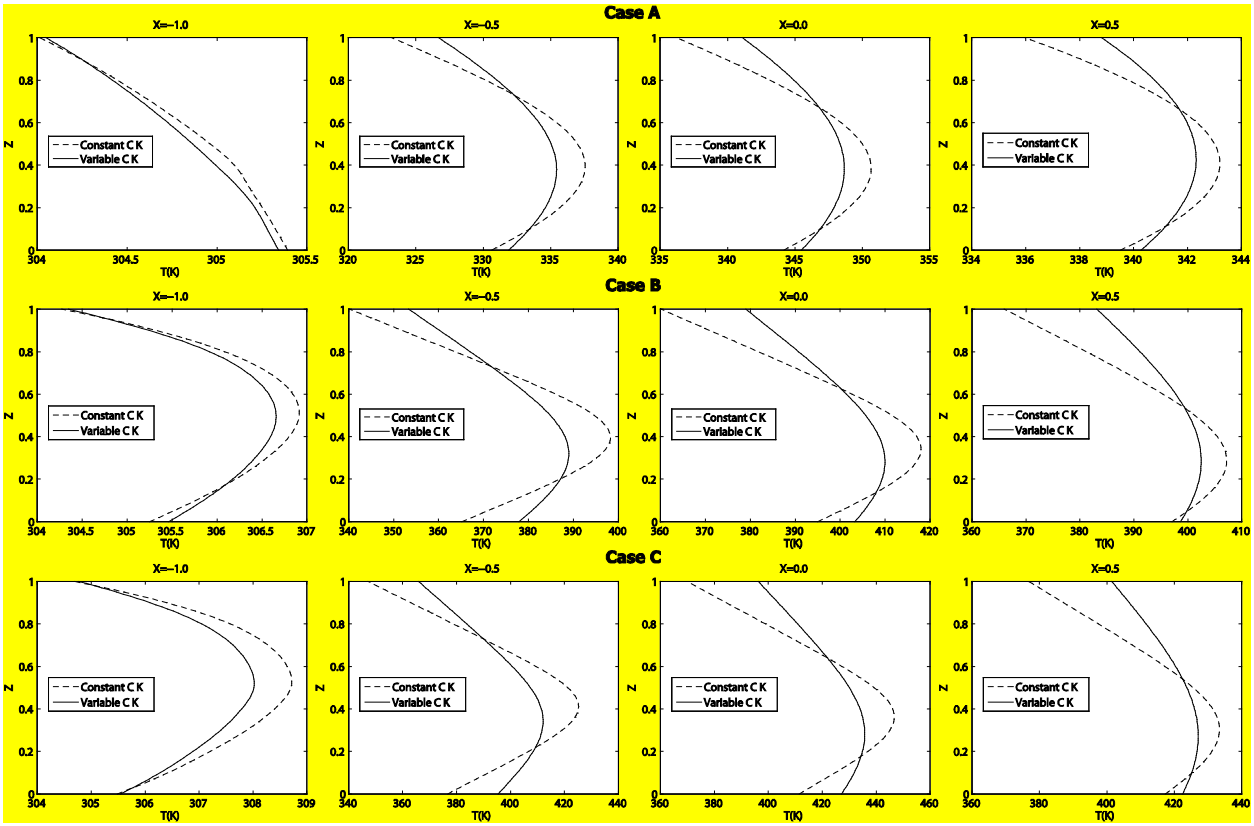

Figure 3: Temperature variations in the lubricant film thickness along the central line of the contact at different X locations

Finally, note that neglecting the temperature and pressure dependence of thermal properties leads to an overestimation of temperature around the midplane of the lubricant film. However, near the solid surfaces temperature is underestimated. This suggests a redistribution of heat from

the middle of the film towards the solid components when thermal properties are allowed to vary with pressure and temperature. This is expected because thermal properties show a global increase throughout the contact as shown in Figures 1 and 2. Hence, a more important heat removal by both conduction and convection is achieved.

4.3 Heat generation and diffusion

Figure 4 shows the total heat generation variations in the film thickness along the central line of the contact for both the “Constant C K” and “Variable C K” cases. The reader is reminded that heat is generated in the lubricant film by two different mechanisms: shear and compression. It is clear that for both the “Constant C K” and “Variable C K” cases, heat generation increases as the lubricant approaches the center of the contact (X=0.0) and then starts decreasing as it moves away from this area. As mentioned previously, this is because of the thin films and high pressures that are encountered in this area, leading to high shear rates and viscosity and thus high generation of heat by shear. Similar to temperature, it is clear that neglecting the temperature and pressure dependence of thermal properties leads to an overestimation of heat generation around the midplane of the film whereas near the solid surfaces, heat generation is underestimated. This explains the higher temperatures that are observed in Figure 3 around the midplane of the lubricant film in the “Constant C K” case. In order to understand this distribution of heat generation in the film thickness it is suggested to observe the lubricant’s velocity variations in the film thickness. These are directly linked to shear rates and thus heat generation by shear throughout the film thickness.

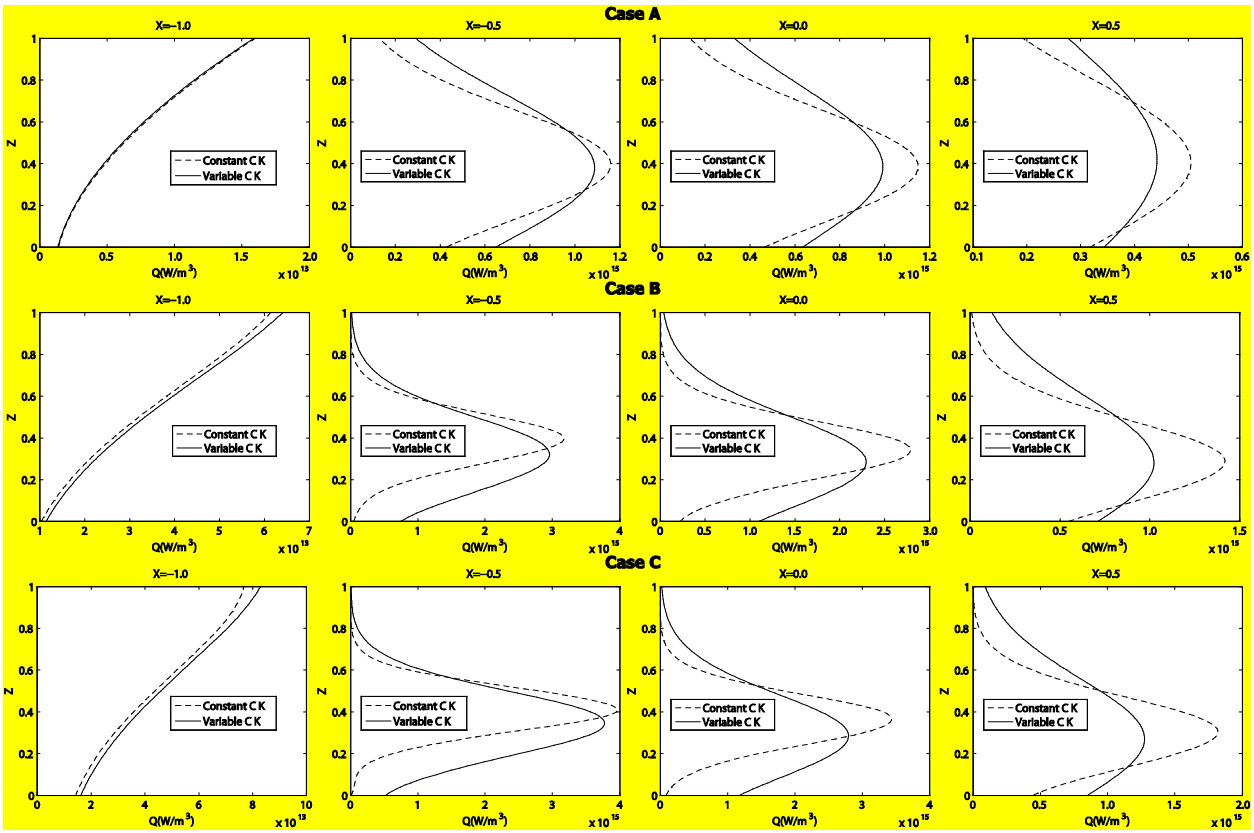

Figure 4: Volumetric heat generation variations in the lubricant film thickness along the central line of the contact at different *X* locations

Figure 5 shows the lubricant flow *x*-velocity component u_f variations in the film thickness along the central line of the contact at different *X* locations. First of all, it is important to note the relatively small velocity gradients with respect to the film thickness (shear rates) near the solid surfaces in the "Constant C K" case. These stem from the lower temperatures that are observed in this case near the solid surfaces (See Figure 3). As a matter of fact, the lower temperatures near the solid surfaces lead to a higher lubricant viscosity and thus a higher resistance to motion, leading to smaller shear rates. This explains, in part, the smaller heat generation observed near the solid surfaces in the "Constant C K" case (See Figure 4). On the other hand, note that, around the midplane of the lubricant film, velocity gradients are more important in the "Constant C K" case, leading to higher shear rates. This explains, in part, the more important heat generation observed in this case around the midplane of the film (See Figure 4). In fact, the amount of volumetric heat generation by shear Q_{shear} inside the lubricant film is expressed as:

$$Q_{shear} = \eta \left[\left(\frac{\partial u_f}{\partial z} \right)^2 + \left(\frac{\partial v_f}{\partial z} \right)^2 \right] \quad (8)$$

Thus, it is clear that heat generation by shear inside the lubricant film is dominated by the shear rate variations raised to the second power. As a consequence, although viscosities near the solid surfaces are expected to be higher in the "Constant C K" case compared to the "Variable C K" case because of the lower temperatures that are observed in this area, heat generation by shear is lower. This is because the latter is dominated by shear rate variations as expressed in equation (8).

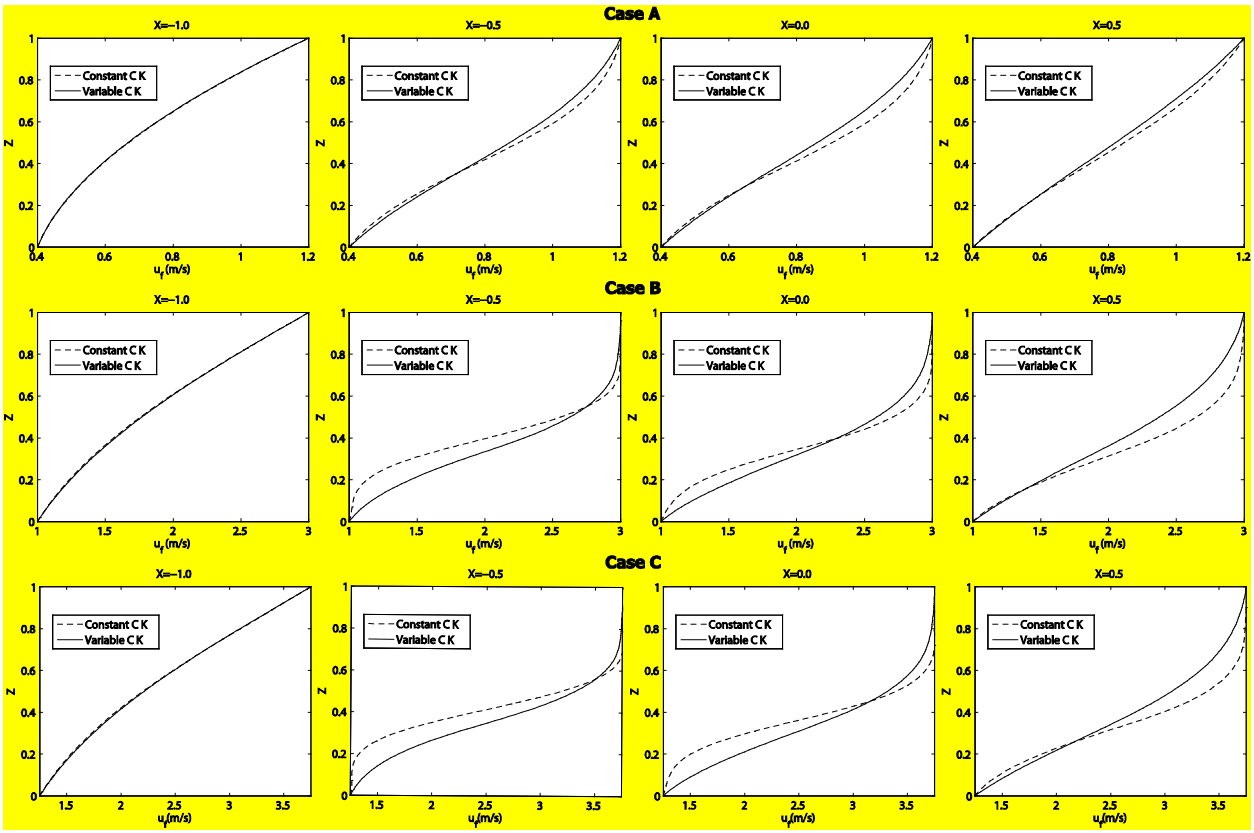

Figure 5: Lubricant flow *x*-velocity component u_f variations in the lubricant film thickness along the central line of the contact at different *X* locations

Finally, computing the heat fluxes at the solid-fluid interfaces confirms the previously discussed redistribution of heat inside the contact. For instance, Figure 6 shows the variations of heat flux *q* as a function of the slide-to-roll ratio (*SRR*) at both solid-fluid interfaces for test case B. It is clear that neglecting the dependence of thermal properties on temperature and pressure leads to an underestimation of the heat fluxes crossing both plane-fluid and sphere-fluid interfaces regardless of the *SRR*. And thus, heat removal from the lubricant film towards the solid components is underestimated. This is expected since heat removal from the lubricant film towards the solid bodies is mainly achieved by conduction. In fact, the fluid velocity in the *z*-direction being neglected, no heat removal is taking place by convection from the lubricant film towards the solids. And since the thermal conductivity of the lubricant is underestimated when it is assumed to be constant (See Figure 1), then heat removal by conduction is underestimated.

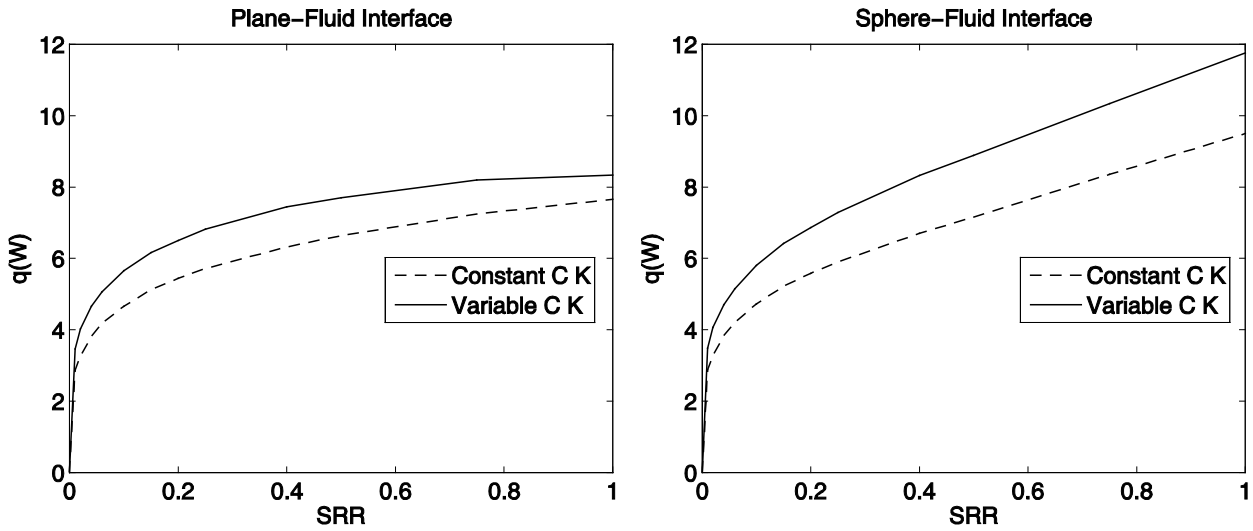

Figure 6: Heat flux variations as a function of *SRR* at the solid-liquid interfaces for test case B

This confirms the redistribution of heat from the midplane of the lubricant film towards the solid surfaces discussed in the previous section.

4.4 Shear stress

Figure 7 shows the shear stress variations in the film thickness along the central line of the contact for both the "Constant C K" and "Variable C K" cases. It is clear that in both cases, shear stresses inside the lubricant film increase as the lubricant approaches the central area of the contact, reaching a maximum at the contact center and then decrease as the lubricant heads towards the exit region. This is to be expected, since viscosity is higher in this area because of the higher pressures that are encountered. In fact, shear stress along the central line of the contact can be simply expressed as:

$$\tau = \eta \frac{\partial u_f}{\partial z} \qquad (9)$$

Since $\partial v_f / \partial z = 0$ along this line. The pressure profile is symmetric with respect to *y* and the surface velocities are unidirectional in the *x*-direction. On the other hand, note that in both the "Variable C K" and "Constant C K" cases, in the central area of the contact shear stresses exhibit very little variations in the film direction. One might tend to think that the limiting shear stress regime is reached. However, a closer examination of the situation reveals that this is only true for Case A. In fact, at *X*=0.0 for instance, the limiting shear stress can be roughly estimated as $\tau_L = \Lambda\ p_h$ (Case A: $\tau_L = 71\,\text{MPa}$, Case B: $\tau_L = 112\,\text{MPa}$, Case C: $\tau_L = 132\,\text{MPa}$). Hence, it is clear that the limiting shear stress is not reached in test cases B and C. What is rather happening is that the more important shear rates around the midplane of the lubricant film are offset by the lower viscosities in this area (incurred by the higher temperatures) leading to an almost flat shear

stress profile in the film thickness. In fact, contrarily to heat generation by shear Q_{shear}, shear stresses τ are equally affected by viscosities and shear rates as suggested by equation (9).

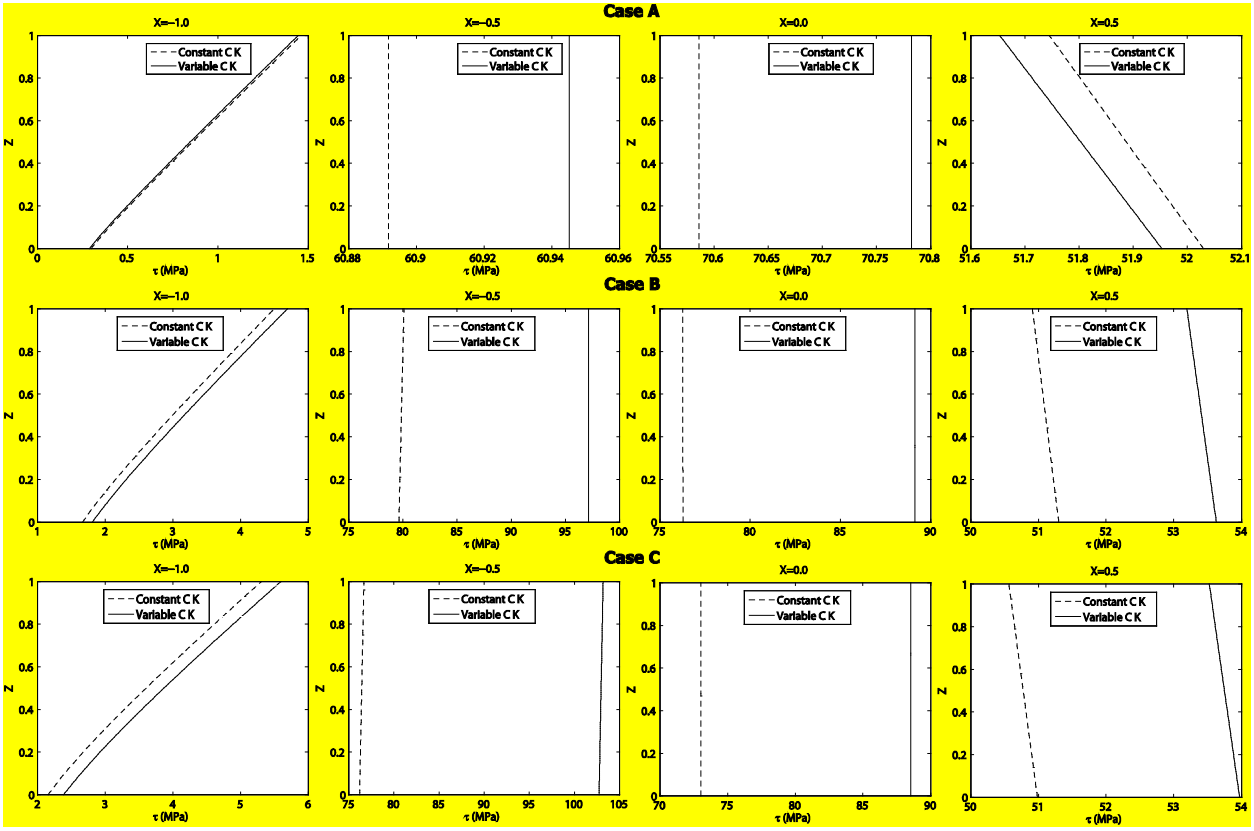

Figure 7: Shear stress variations in the lubricant film thickness along the central line of the contact at different *X* locations

Finally, note that all throughout the contact, shear stresses are greater in the "Variable C K" case compared to the "Constant C K" one (except at the inlet and exit of the contact in Case A where thermal effects are less important), leading to higher friction coefficients in the former case.

5. Discussion

The results of the local investigation discussed in section 3 shed the light on the global observations made in [11]. As a matter of fact, in [11] it was observed that neglecting the dependence of lubricant thermal properties on pressure and temperature had little effect on film thickness under pure-rolling conditions, whereas it lead to underestimating friction coefficients at high *SRR*. Figure 8 shows the traction curves for the same loading and mean entrainment speed conditions of cases A, B and C, while sliding speed is varied to cover a range of *SRR* going from 0 to 1. It is clear that, at high *SRR* or/and high load and high mean entrainment speed conditions, friction coefficients are underestimated in the "Constant C K" case.

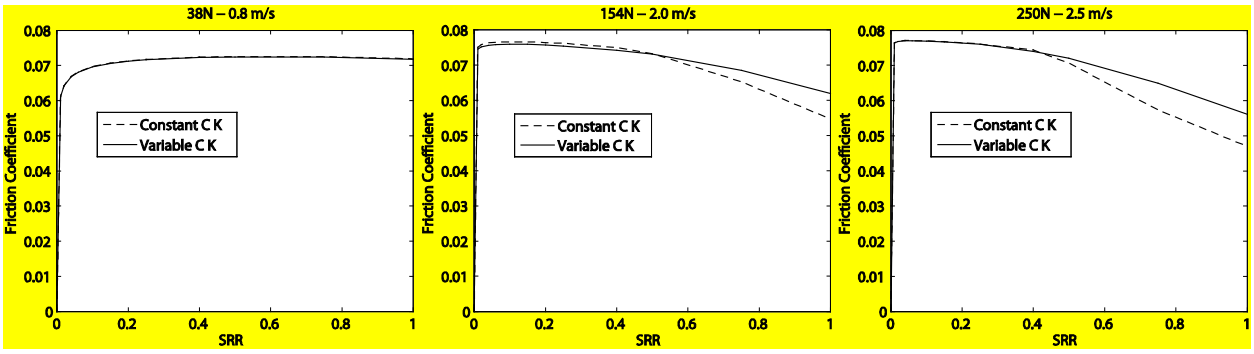

Figure 8: Traction curves as a function of slide-to-roll ratio (*SRR*) for a steel-steel circular contact under loading and mean entrainment speed conditions of test cases A, B and C

The results of section 3 clearly suggest that both thermal conductivity and volumetric heat capacity of the lubricant exhibit a significant increase as the lubricant passes through the contact. Thermal conductivity dictates heat transfer by conduction within the lubricant film whereas convection inside the film is dictated by the volumetric heat capacity of the lubricant. Thus, neglecting the variation of lubricant thermal properties with pressure and temperature leads to an underestimation of heat removal by the lubricant from the contact area towards the environment. In fact, heat is removed by convection towards the exit of the contact, whereas it is removed by conduction towards the solid components as well as the inlet and exit areas of the contact. Hence, neglecting the pressure and temperature dependence of thermal properties leads to globally higher temperatures inside the contact, leading to lower shear stresses and thus lower friction coefficients. All in all, it is clear that, allowing thermal properties of the lubricant to vary with pressure and temperature leads to a redistribution of heat from the center of the contact towards the surroundings (solid components and inlet and exit areas of the contact). Finally, note that this observation only affects the traction behavior under high *SRR* or/and high load and high mean entrainment speed conditions, in other words, under high thermal dissipation regime. In Figure 8, there is practically no difference between the traction curves of the "Constant C K" and "Variable C K" cases up to *SRR*≈0.5. Furthemore, for the loading and mean entrainment speed conditions of test case A (Figure 8, Left), the difference is negligible over the entire considered range of SRR. In fact, at low *SRR* or/and load and mean entrainment speed (low thermal dissipation regime), heat generation is relatively small and the traction behavior is dominated by the Limiting Shear Stress of the lubricant rather than thermal effects (in fact, at SRR=1.0 the Limiting Shear Stress was only reached for test case A as seen in section 4.4). However, under high *SRR* regime or/and high load and high mean entrainment speed conditions (high thermal dissipation regime), the amount of heat generated inside the contact becomes relatively important leading to relatively high lubricant temperatures. This leads to significant reduction in the viscosity of the lubricant, thus preventing the stress from reaching its limiting value as discussed in section 4.4. Hence, under this regime, traction behavior is dominated by thermal effects rather than the Limiting Shear Stress of the lubricant.

6. Conclusion

This work presents a quantitative numerical investigation of the local behavior of TEHL highly loaded contacts. Three different test cases are considered over a considerable range of load and mean entrainment speed conditions. The numerical model employed in this work has the particularity of using rheological models stemming from measured transport properties including viscosity. Only the limiting stress was obtained from a contact measurement. A particular emphasis is placed on the pressure and temperature dependence of the lubricant thermal properties. It is shown that neglecting this dependence has a local effect on the different parameters governing the behavior of the contact: temperature, viscosity, shear rates, heat generation… On a more global level, this leads to an underestimation of friction coefficients under high thermal dissipation regime where the traction behavior of the contact is dominated by thermal effects rather than the Limiting Shear Stress of the lubricant. This observation was found to stem from the fact that thermal properties of the lubricant (when allowed to vary) exhibit an important increase as the lubricant flows into the contact. This enhances heat removal by the lubricant from the contact area towards the surrounding (inlet and exit areas of the contact as well as the solid components). Hence, a redistribution of heat from the center of the contact towards the outside is taking place, leading to globally lower temperatures inside the contact, which leads to higher shear stresses and thus higher friction coefficients.

Acknowledgments

Dr. Bair was supported by the Center for Compact and Efficient Fluid Power, a National Science Foundation Engineering Research Center funded under cooperative agreement number EEC-0540834.
The fifth author wishes to thank Mr. A. de Vries, Director SKF Group Product Development, for his kind permission to publish this article.

Nomenclature

ρ : Lubricant's density
ρ_R : Lubricant's density at reference state
η : Lubricant's Generalized Newtonian viscosity
μ : Lubricant's viscosity
τ : Shear stress
τ_L : Limiting shear stress
a : Hertzian contact radius
c : Lubricant's heat capacity
c_0 : Lubricant's ambient heat capacity
C : Lubricant's volumetric heat capacity
C_0 : Lubricant's ambient volumetric heat capacity
k : Lubricant's thermal conductivity
k_0 : Lubricant's ambient thermal conductivity

L : Contact's external applied load
p : Pressure
p_h : Hertzian contact pressure
q : Heat flux at solid-liquid interfaces
Q : Volumetric heat generation
Q_{shear} : Volumetric heat generation by shear
SRR : Slide-to-Roll ratio $=(u_s-u_p)/u_m$
T : Temperature
T_0 : Ambient temperature
T_R : Reference temperature
u_f , v_f : Lubricant flow velocity components in the *x and y* directions respectively
u_m : Mean entrainment speed
u_s : Sphere's surface velocity
u_p : Plane's surface velocity
V : Volume
V_R : Volume at reference state
x,y,z : Space coordinates
X,Y,Z : Dimensionless space coordinates ($X = x/a$, $Y = y/a$, $Z = z/a$)

References

[1] Barus C. – Isothermal, Isopiestics and Isometrics Relative to viscosity, *Am. J. Sci.*, 1893, vol. 45, pp. 87-96.

[2] Roelands C. J. A. – Correlational aspects of the Viscosity-Temperature-Pressure Relationship of Lubricating Oils, *PhD Thesis*, Technische Hogeschool Delft, The Netherlands, 1966.

[3] Eyring H. – Viscosity, Plasticity and Diffusion as Examples of Absolute Reaction Rates, *J. Chem. Phys.*, 1936, vol. 4, pp. 283-291.

[4] Bair S. – High Pressure Rheology for Quantitative Elastohydrodynamics, *Elsevier Science*, Amsterdam, 2007.

[5] Kioupis L. I. and Maginn E. J. - Molecular Simulation of Poly-alpha-olefin Synthetic Lubricants: Impact of Molecular Architecture on Performance Properties, *J. Phys. Chem. (B)*, 1999, vol. 103, pp. 10781-10790.

[6] Tanner R. I. – Engineering Rheology, second edition, *Oxford University Press*, Oxford, 2000, p. 229.

[7] Bair S. and McCabe C. - A Study of Mechanical Shear Bands in Liquids at High Pressure, *Trib. Intern.*, 2004, vol. 37, pp. 783-789.

[8] Bair S. – Reference Liquids for Quantitative Elastohydrodynamics: Selection and Rheological Characterization, *Tribology Letters*, 2006, vol. 22, pp. 197-206.

[9] Habchi. W., Eyheramendy D., Bair S., Vergne P. and Morales-Espejel G. – Thermal Elastohydrodynamic Lubrication of Point Contacts Using a Newtonian / Generalized Newtonian Lubricant, *Tribology Letters*, 2008, vol. 30 (1), pp. 41-52.

[10] Chang L., Qu S., Webster M.N. and Jackson A. – On the Mechanisms of the Reduction in EHL Traction at Low Temperature, *Tribology Transactions*, 2006, vol. 49 (2), pp. 182-191.

[11] W. Habchi, P. Vergne, S. Bair, O. Andersson, D. Eyheramendy and G. E. Morales-Espejel – Influence of Pressure and Temperature Dependence of Thermal Properties of a Lubricant on the Behaviour of Circular TEHD Contacts, *Tribology International*, 2010, vol. 43, pp. 1842-1850.

[12] Campos A., Sottomayor A. and Seabra J. – Non-Newtonian Thermal Analysis of an EHD Contact Lubricated with MIL-L-23699 Oil, *Tribology International*, 2006, vol. 39 (12), pp. 1732-1744.

[13] Sharif K.J, Kong S., Evans H.P. and Snidle R.W. - Contact and Elastohydrodynamic Analysis of Worm Gears. Part 1: Theroretical Formulation, *Proc. IMechE, Part C, J. Mech. Eng. Sci*, 2001, vol. 215 (7)**,** pp. 817-830.

[14] Sharif K.J, Kong S., Evans H.P. and Snidle R.W. - Contact and Elastohydrodynamic Analysis of Worm Gears. Part 2: Results, *Proc. IMechE, Part C, J. Mech. Eng. Sci*, 2001, vol. 215 (7)**,** pp. 831-846.

[15] Larsson R., Larsson P. O., Eriksson E., Sjöberg M. and Höglund E. - Lubricant Properties for Input to Hydrodynamic and Elastohydrodynamic Lubrication Analyses, *Proc. IMechE, Part J, J. Engnrng. Trib.*, 2000, vol. 214 (1), pp. 17-27.

[16] Hersey M. D. and Zimmer J. C. - Heat Effects in Capillary Flow at High Rates of Shear, *J. Applied Phys.*, 1937, vol. 8, pp. 359-363.

[17] Murnaghan, F.D., 1944, "The Compressibility of Media under Extreme Pressures", *Proceedings of the National Academy of Sciences*, Vol. 30, p. 244-247.

[18] Bair, S., 2004, "A Rough Shear Thinning Correction for EHD Film Thickness", *STLE Tribology Trans.*, Vol. 47, N°3, p. 361-365.

[19] Habchi W. – A Full-System Finite Element Approach to Elastohydrodynamic Lubrication Problems: Application to Ultra-Low-Viscosity Fluids, *PhD Thesis*, 2008, INSA de Lyon, France.

[20] Habchi W., Eyheramendy D., Vergne P. and Morales-Espejel G. – Stabilized Fully-Coupled Finite Elements for Elastohydrodynamic Lubrication Problems, *Advances in Engineering Software*, (Article In Press).

[21] Yang, P., Wen, S. - A Generalized Reynolds Equation for Non-Newtonian Thermal Elastohydrodynamic Lubrication. *ASME Journal of Tribology*, 1990, vol. 112, pp. 631-636.